Magnetized astrophysical jets

Nektarios Vlahakis
University of Athens

Outline

- linear stability analysis of cylindrical jets
  - kink instability in relativistic, cold, magnetized flows
  - growth rate and its dependence on σ and B_ϕ/B_z
- Rarefaction acceleration
  - the 2D relativistic magnetized case
    - simple waves
    - steady-state flow around a corner
  - the 3D axisymmetric case

Observations: jet speed

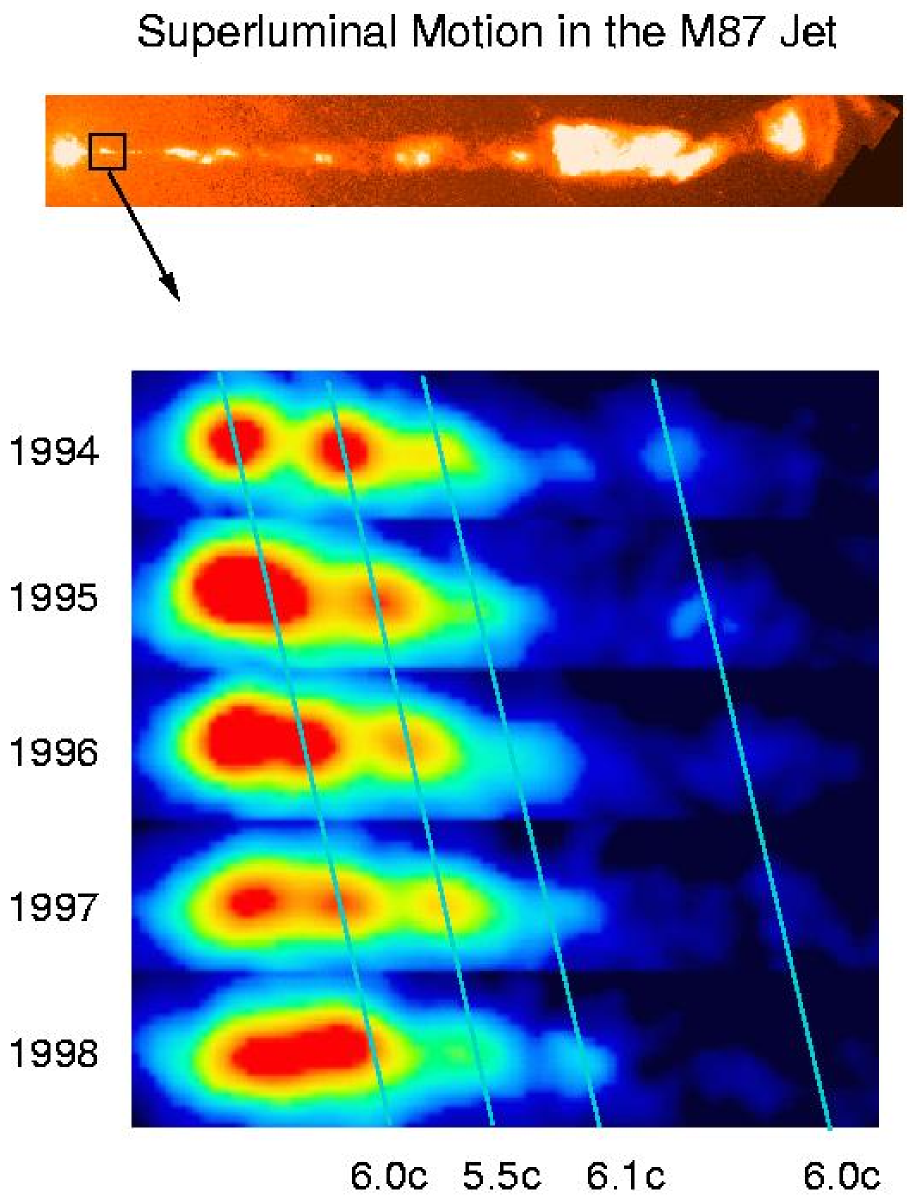

Polarization

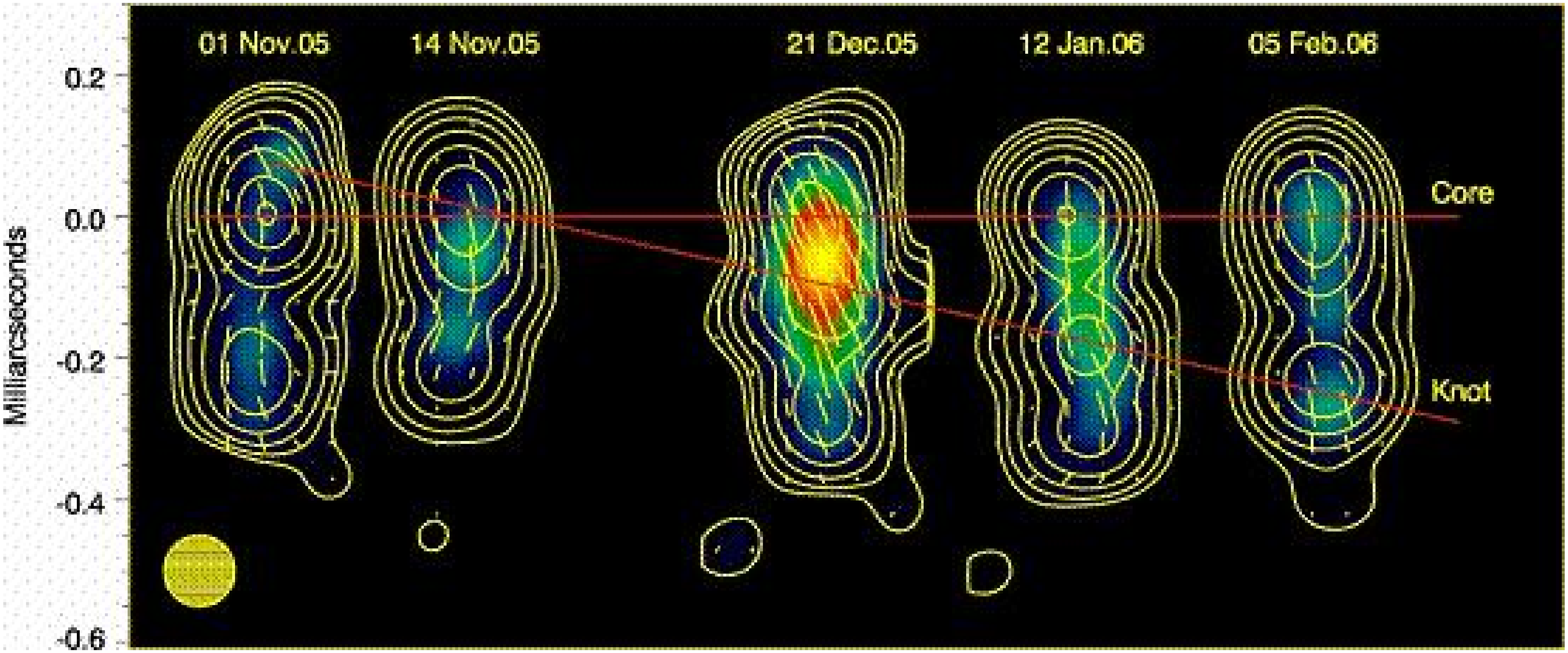

(Marscher et al)

helical motion and field rotate the EVPA as the blob moves

observed $\boldsymbol{E}_{rad} \perp \boldsymbol{B}_{rad}$ and $\boldsymbol{B}_{rad}$ is $\parallel$ $\boldsymbol{B}_{\perp los}$
(modified if the jet is relativistic)

Faraday RM gradients across the jet

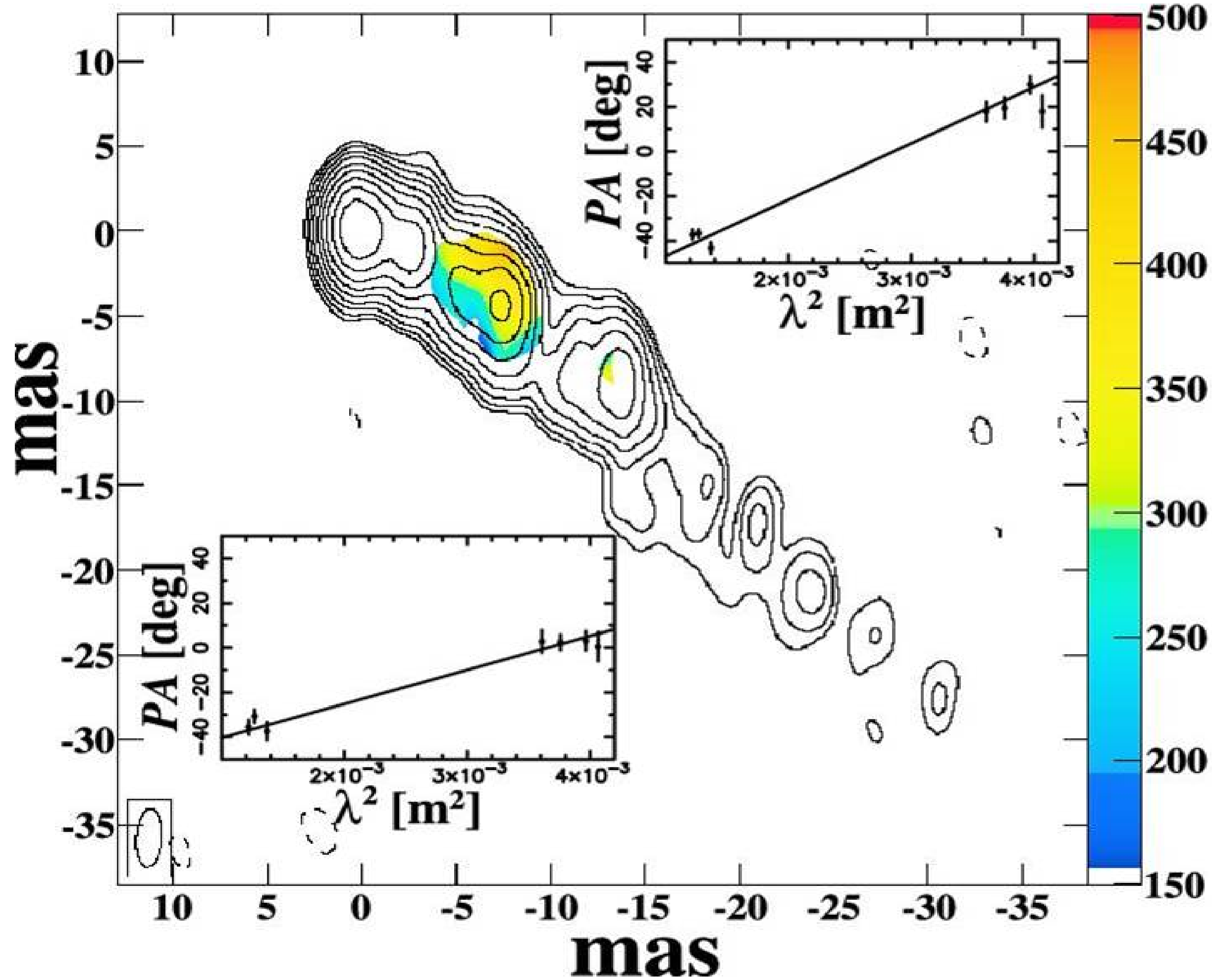

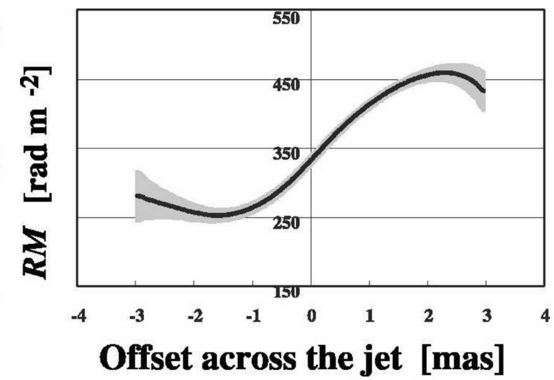

(from Asada et al)

helical field surrounding the emitting region

Relativistic motion in GRB jets

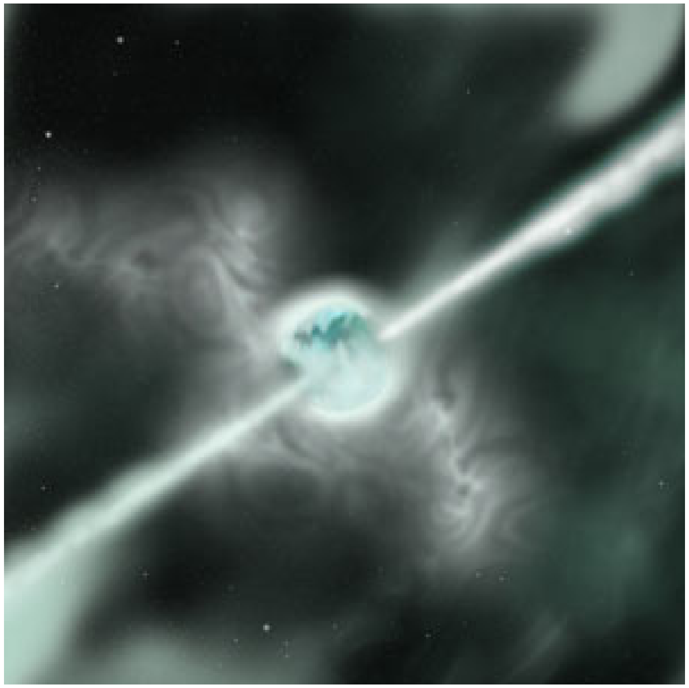

the only solution to the “compactness problem”

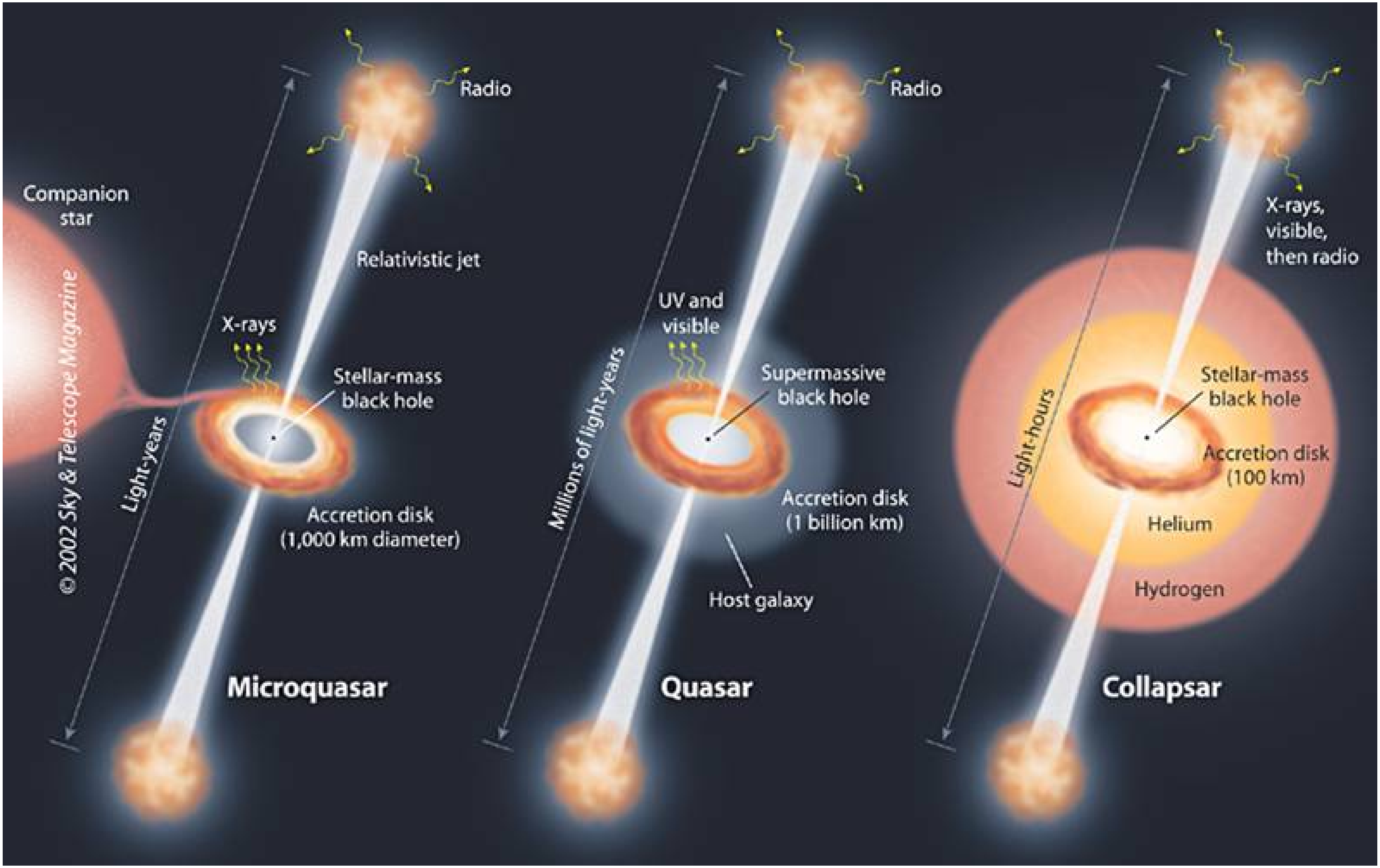

Radio
Companion star
Relativistic jet
X-rays
Stellar-mass black hole
© 2002 Sky & Telescope Magazine
Light-years
Accretion disk (1,000 km diameter)
Microquasar
Radio
UV and visible
Supermassive black hole
Millions of light-years
Accretion disk (1 billion km)
Host galaxy
Quasar
X-rays, visible, then radio
Stellar-mass black hole
Light-hours
Accretion disk (100 km)
Helium
Hydrogen
Collapsar

Linear stability of relativistic jets

Unperturbed relativistic cylindrical jet

helical, axisymmetric, cylindrically symmetric and steady flow

$$\boldsymbol{V}_0 = V_{0z}(\varpi)\hat{z} + V_{0\phi}(\varpi)\hat{\phi}\,, \quad \gamma_0 = \gamma_0(\varpi) = (1 - V_{0z}^2 - V_{0\phi}^2)^{-1/2}\,,$$

$$\boldsymbol{B}_0 = B_{0z}(\varpi)\hat{z} + B_{0\phi}(\varpi)\hat{\phi}\,, \quad \boldsymbol{E}_0 = (V_{0z}B_{0\phi} - V_{0\phi}B_{0z})\hat{\varpi}\,,$$

$$\rho_{00} = \rho_{00}(\varpi)\,, \quad \xi_0 = \xi_0(\varpi)\,, \quad \Pi_0 = \frac{\Gamma - 1}{\Gamma}(\xi_0 - 1)\,\rho_{00} + \frac{B_0^2 - E_0^2}{2}\,.$$

Equilibrium condition $$\frac{B_{0\phi}^2 - E_0^2}{\varpi} - \xi_0\rho_{00}\frac{\gamma_0^2 V_{0\phi}^2}{\varpi} + \frac{d\Pi_0}{d\varpi} = 0\,.$$

The jet is expected to be unstable to current-driven instabilities (Kruskal-Shafranov) — role of inertia?

Linearized equations

$$Q(\varpi\,,z\,,\phi\,,t) = Q_0(\varpi) + Q_1(\varpi)\exp\left[i(m\phi + kz - \omega t)\right]$$

$$\left(\begin{array}{c} 10\times 12 \text{ array} \\ \text{function of } \varpi\,,\omega\,,k \end{array}\right)\begin{pmatrix} \gamma_1 \\ \rho_{01} \\ B_{1z} \\ B_{1\phi} \\ iB_{1\varpi} \\ \xi_1 \\ V_{1z} \\ V_{1\phi} \\ d\left(i\varpi V_{1\varpi}\right)/d\varpi \\ d\Pi_1/d\varpi \\ i\varpi V_{1\varpi} \\ \Pi_1 \end{pmatrix} = 0$$

reduces to (4 equations in real space)

$$\frac{d}{d\varpi}\left(\begin{array}{c} y_1 \\ y_2 \end{array}\right) + \frac{1}{\mathcal{D}}\left(\begin{array}{cc} \mathcal{F}_{11} & \mathcal{F}_{12} \\ \mathcal{F}_{21} & \mathcal{F}_{22} \end{array}\right)\left(\begin{array}{c} y_1 \\ y_2 \end{array}\right) = 0\,,$$

where the (complex) unknowns are

$$y_1 = i\frac{\varpi V_{1\varpi}}{\omega_0}\,, \qquad y_2 = \Pi_1 + \frac{y_1}{\varpi}\frac{d\Pi_0}{d\varpi}$$

($\mathcal{D}\,, \mathcal{F}_{ij}$ are determinants of 10×10 arrays).

Equivalently

$$y_2'' + \left[\frac{\mathcal{F}_{11} + \mathcal{F}_{22}}{\mathcal{D}} + \frac{\mathcal{F}_{21}}{\mathcal{D}}\left(\frac{\mathcal{D}}{\mathcal{F}_{21}}\right)'\right] y_2' + \left[\frac{\mathcal{F}_{11}\mathcal{F}_{22} - \mathcal{F}_{12}\mathcal{F}_{21}}{\mathcal{D}^2} + \frac{\mathcal{F}_{21}}{\mathcal{D}}\left(\frac{\mathcal{F}_{22}}{\mathcal{F}_{21}}\right)'\right] y_2 = 0\,,$$

which for uniform flows with $V_{0\phi} = 0$, $B_{0\phi} = 0$, reduces to Bessel.

Eigenvalue problem

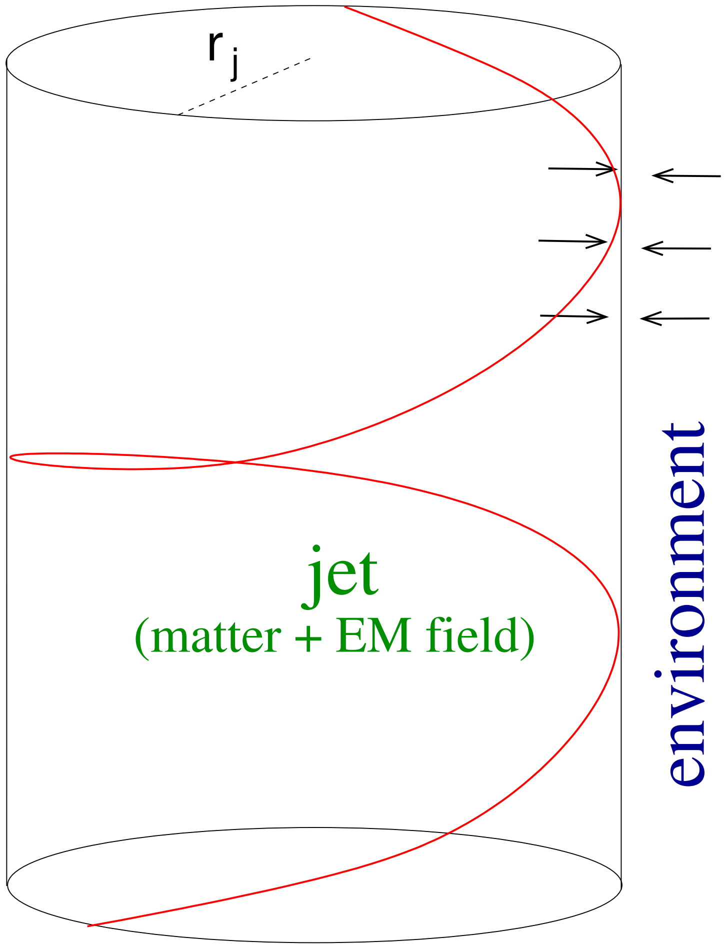

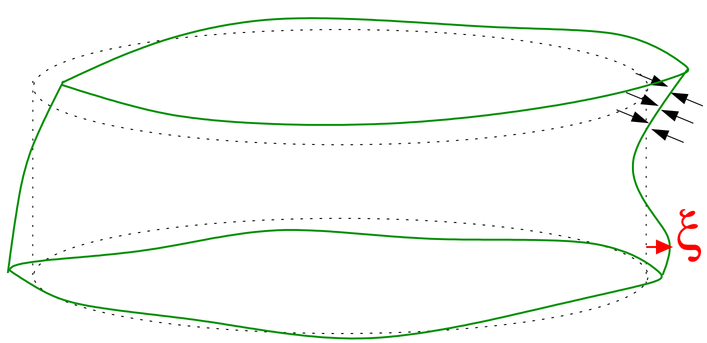

- solve the problem inside the jet (attention to regularity condition on the axis)

- similarly in the environment (solution vanishes at ∞)

- Match the solutions at r_j:

$[\![y_1]\!] = 0\,, [\![y_2]\!] = 0 \longrightarrow$ dispersion relation

$\star$ spatial approach: $\omega = \Re\omega$ and $\Re k = \Re k(\omega), \Im k = \Im k(\omega)$

$Q = Q_0(\varpi) + Q_1(\varpi)e^{-\Im k z}e^{i(m\phi + \Re k z - \omega t)}$

$\star$ temporal approach: $k = \Re k$ and $\Re\omega = \Re\omega(k), \Im\omega = \Im\omega(k)$

$Q = Q_0(\varpi) + Q_1(\varpi)e^{\Im\omega t}e^{i(m\phi + kz - \Re\omega t)}$

Unperturbed jet solutions

Try to mimic the Komissarov et al simulation results
(for AGN and GRB jets)

- cold, nonrotating jet

$$\boldsymbol{V}_0 = V_0(\varpi)\hat{z}\,, \quad \gamma_0 = \gamma_0(\varpi) = (1 - V_0^2)^{-1/2}\,,$$

$$\boldsymbol{B}_0 = B_{0z}(\varpi)\hat{z} + B_{0\phi}(\varpi)\hat{\phi}\,, \quad \boldsymbol{E}_0 = V_0 B_{0\phi}\hat{\varpi}\,,$$
$$\rho_{00} = \rho_{00}(\varpi)\,, \quad \xi_0 = 1\,.$$

- Equilibrium condition

$$\frac{B_{0\phi}^2/\gamma_0^2}{\varpi} + \frac{d}{d\varpi}\left(\frac{B_{0z}^2 + B_{0\phi}^2/\gamma_0^2}{2}\right) = 0\,,$$

relates B_{0z} with $B_{0\phi}/\gamma_0$.

A cold, nonrotating solution:

$$B_{0z} = \frac{B_j}{\left[1+(\varpi/\varpi_0)^2\right]^\zeta}\,, \qquad B_{0\phi} = -\gamma_0 B_{0z}\sqrt{\frac{\left[1+(\varpi/\varpi_0)^2\right]^{2\zeta}-1-2\zeta(\varpi/\varpi_0)^2}{(2\zeta-1)(\varpi/\varpi_0)^2}}\,.$$

ϖ_0 , ζ free parameters, γ_0 , ρ_{00} free functions.

- choice of ζ:

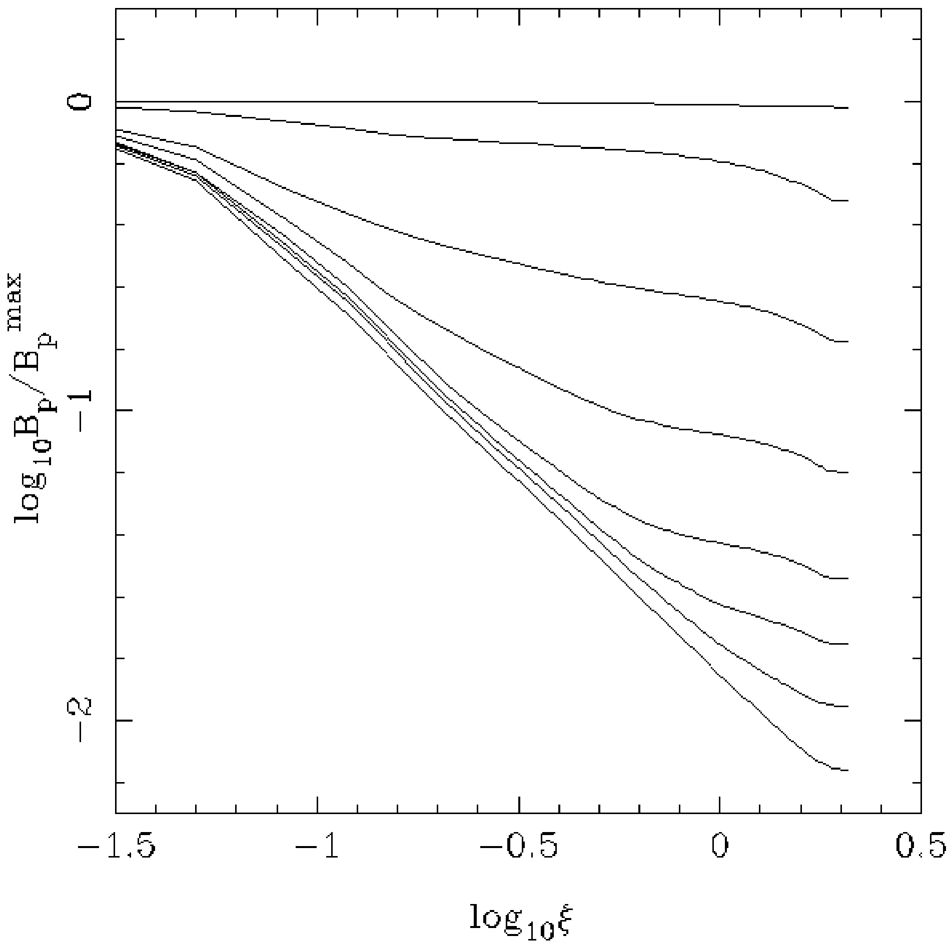

$$B_{0z} \propto \varpi^{-1.2}$$

$$\zeta = 0.6$$

Formation of core crucial for the acceleration.

The bunching function $\mathcal{S} \equiv \dfrac{\overbrace{\pi\varpi^2}^{S} B_{0z}}{\int_0^{\varpi} B_{0z} \underbrace{2\pi\varpi d\varpi}_{dS}}$ is related to the acceleration efficiency $\sigma = \dfrac{1}{\frac{\mathcal{S}_f}{\mathcal{S}} - 1}$, where $\mathcal{S}_f$ integral of motion ~ 0.9.

Since $\mathcal{S} \approx 1 - \zeta$ we get $\sigma = \dfrac{1-\zeta}{\zeta - 0.1}$.

- choice of $\gamma_0(\varpi)$:

From Ferraro's law $V_{0\phi} = \varpi\Omega + V_{0z}B_{0\phi}/B_{0z}$, where Ω integral of motion, we get $-B_{0\phi}/B_{0z} \approx \varpi\Omega$, or,

$$\gamma_0 \approx \varpi\Omega \sqrt{\frac{(2\zeta-1)(\varpi/\varpi_0)^2}{\left[1+(\varpi/\varpi_0)^2\right]^{2\zeta} - 1 - 2\zeta(\varpi/\varpi_0)^2}}.$$

The choice of ϖ_0, $\Omega(\varpi)$ control the pitch $B_{0\phi}/(\varpi B_{0z})$, and the values of γ_0 on the axis and the jet surface.

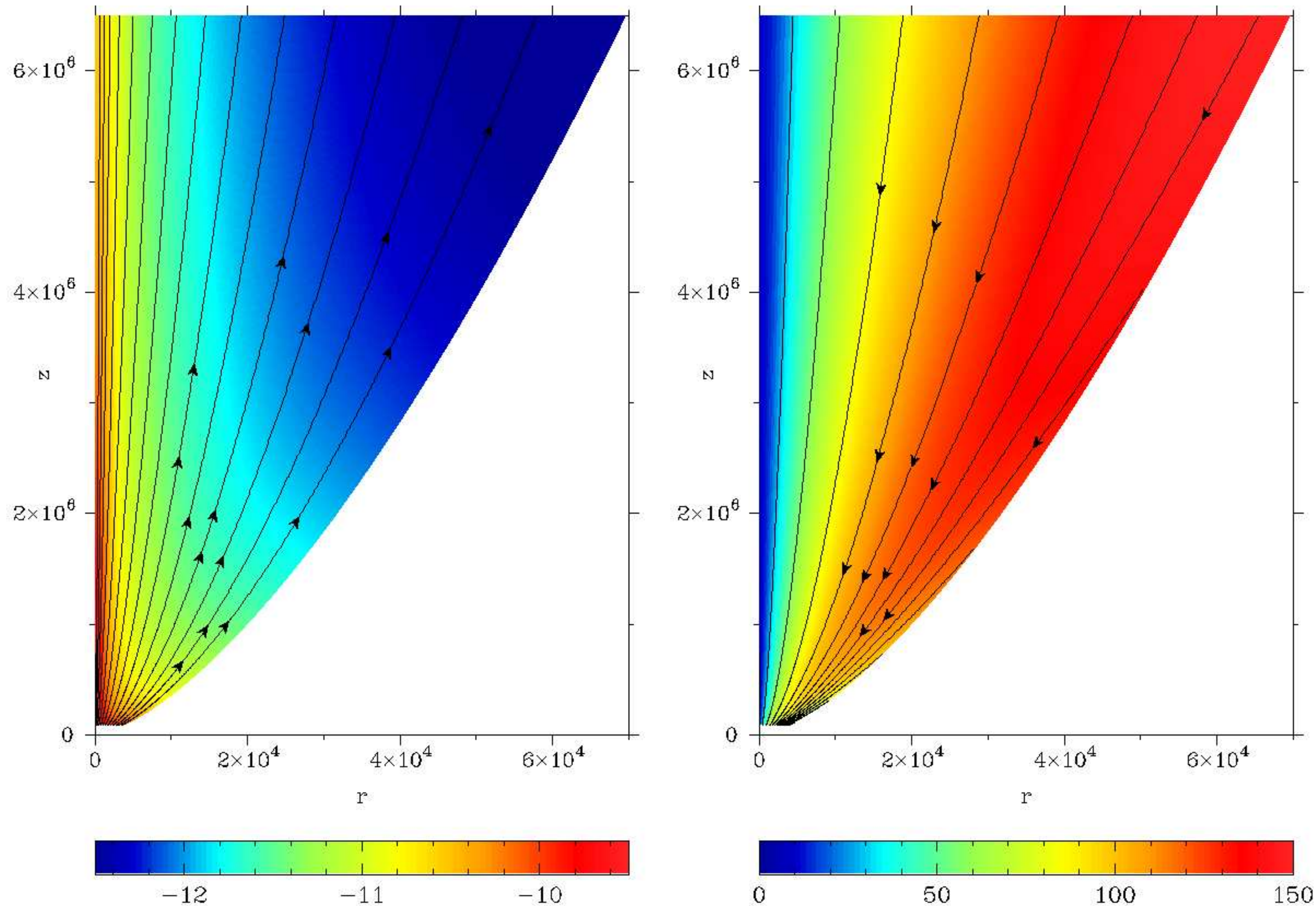

left: density/field lines, right: Lorentz factor/current lines (jet boundary $z \propto r^{1.5}$)
Uniform rotation $\rightarrow \gamma$ increases with r

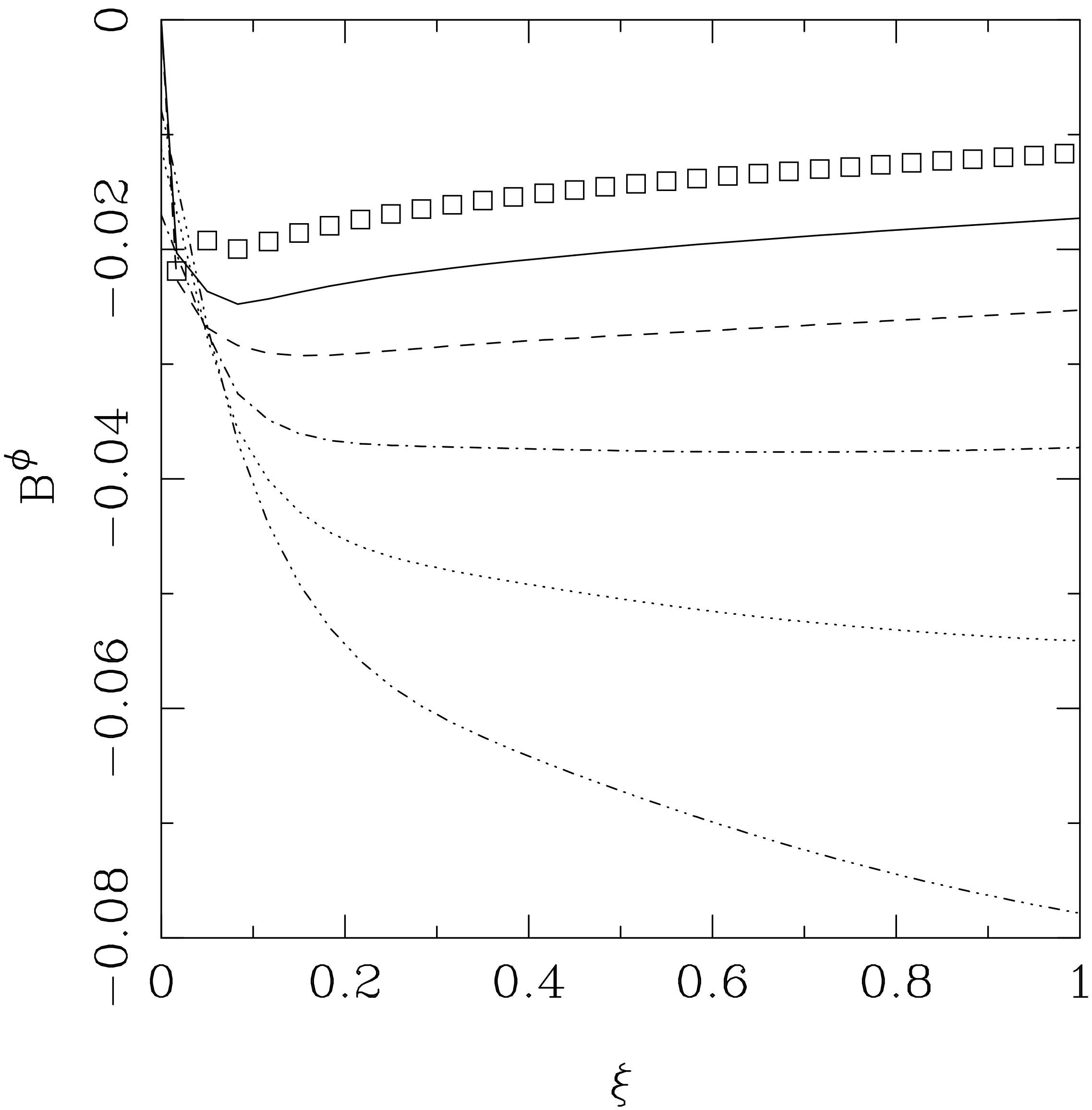

0
−0.02
−0.04
−0.06
−0.08
B^{ϕ}
0
0.2
0.4
0.6
0.8
1
ξ

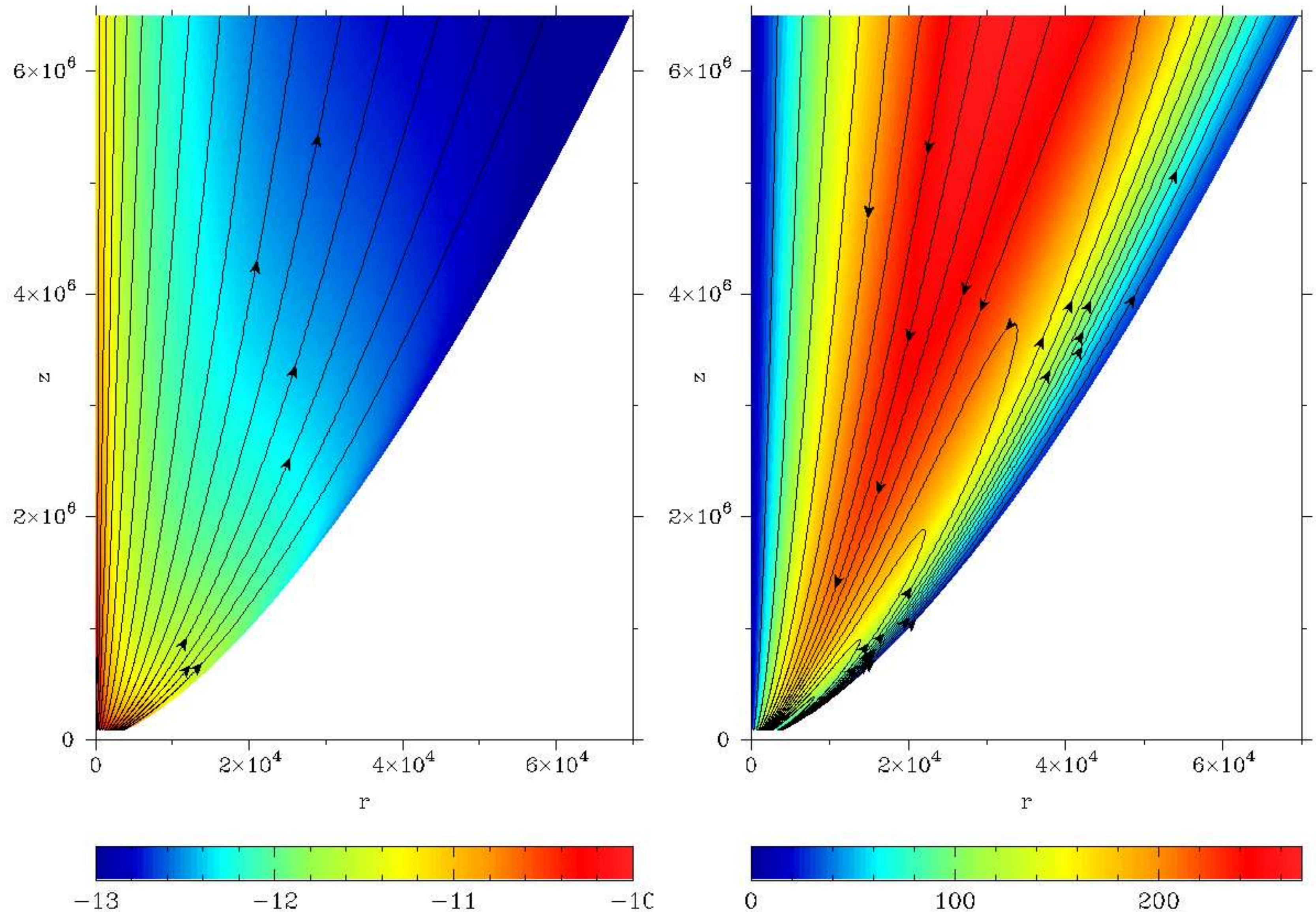

Differential rotation → slow envelope and faster decrease of B_ϕ

- choice of $\rho_{00}(\varpi)$:

This comes from the mass-to-magnetic flux ratio integral $\frac{\gamma_0 \rho_{00} V_0}{B_{0z}}$, which is assumed constant in the simulations. So $\rho_{00} \propto B_{0z}/\gamma_0$.
The constant of proportionality from the value of
$\sigma = \left. \frac{B_{0\phi}^2/\gamma_0^2}{\rho_{00}} \right|_{\varpi=\varpi_j}$.

- external medium:

uniform, static, with zero $B_{0\phi}$ and $V_{0\phi} \rightarrow$ Bessel.
In all the following a thermal pressure is assumed, $\xi_e = 1.01$.
A cold, magnetized environment gives approximatelly same results.

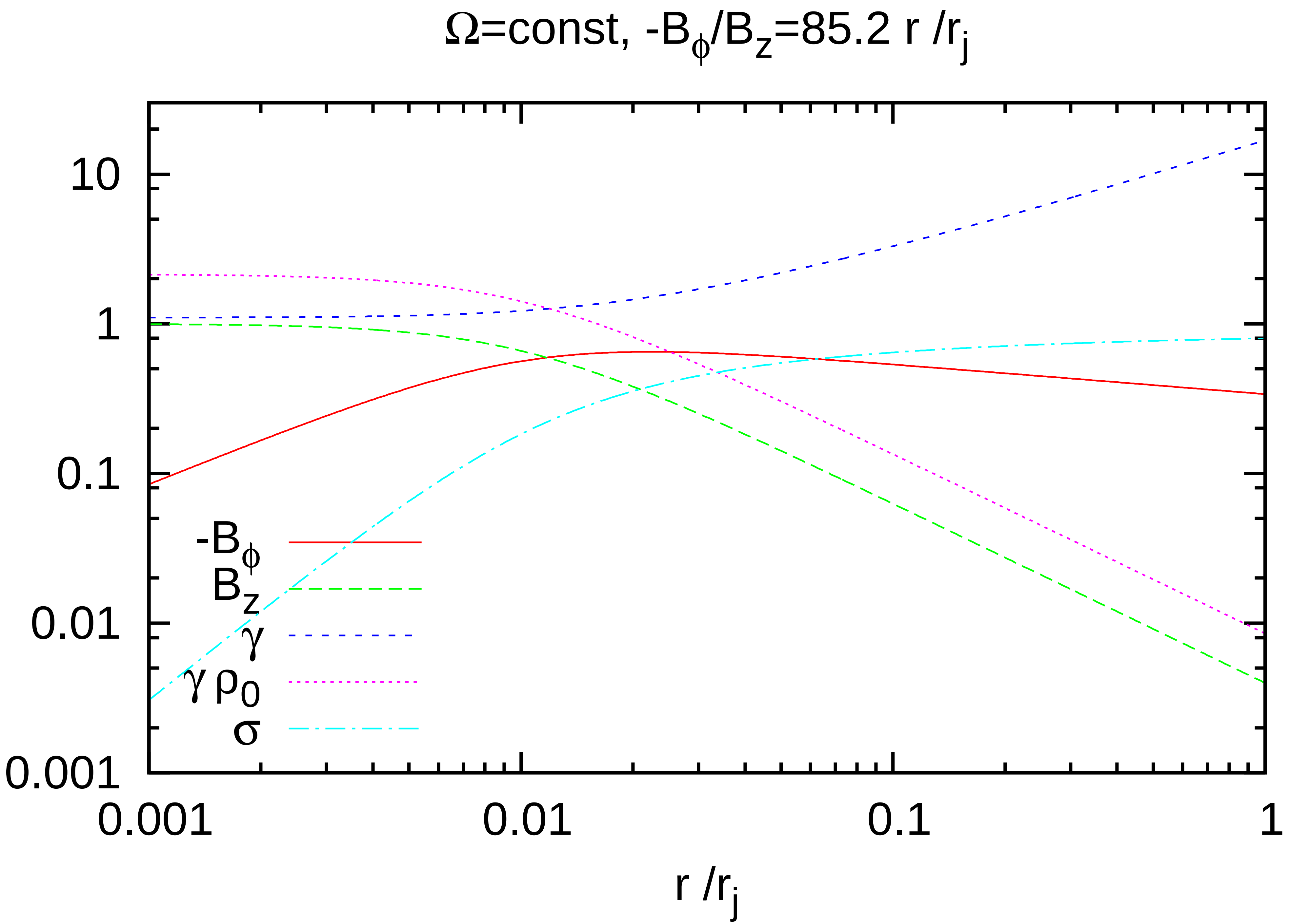

Ω=const, -B_φ/B_z=85.2 r /r_j
10
1
0.1
0.01
0.001
0.001
0.01
0.1
1
r /r_j
-B_φ
B_z
γ
γ ρ_0
σ

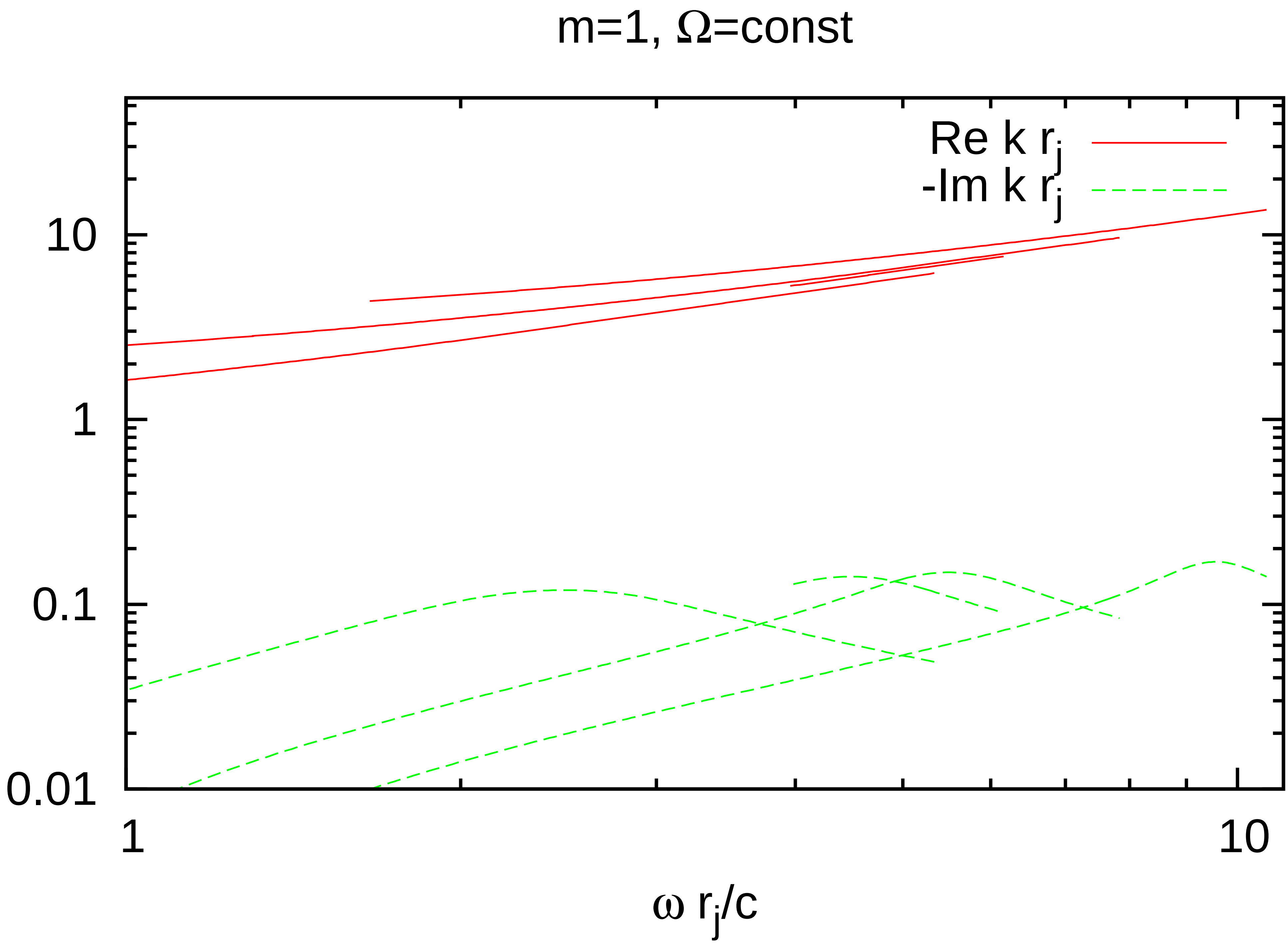
m=1, Ω=const
Re k r_j
-Im k r_j
10
1
0.1
0.01
1
10
ω r_j/c

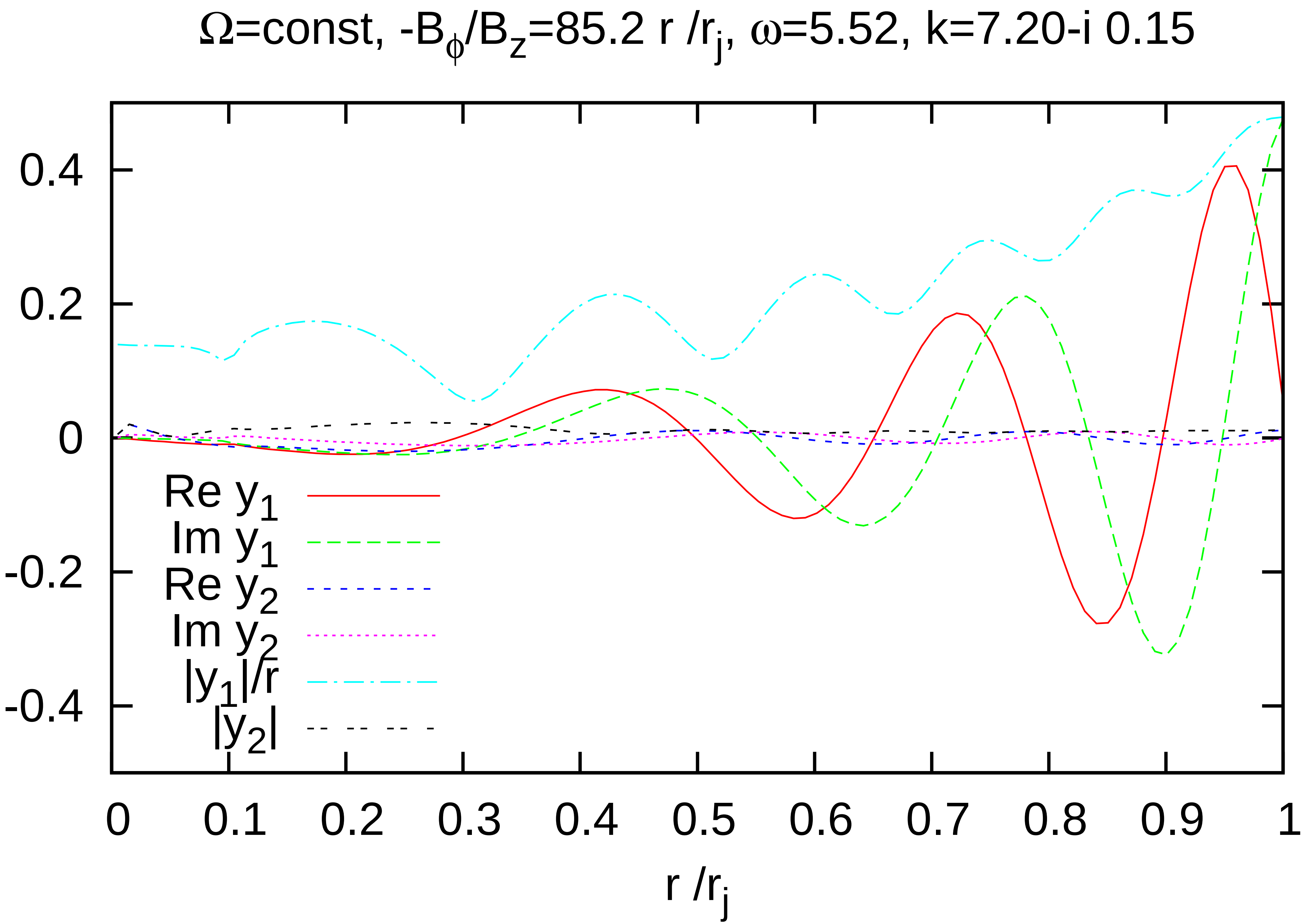
Ω=const, -B_φ/B_z=85.2 r /r_j, ω=5.52, k=7.20-i 0.15
0.4
0.2
0
-0.2
-0.4
Re y1
Im y1
Re y2
Im y2
|y1|/r
|y2|
0
0.1
0.2
0.3
0.4
0.5
0.6
0.7
0.8
0.9
1
r /r_j

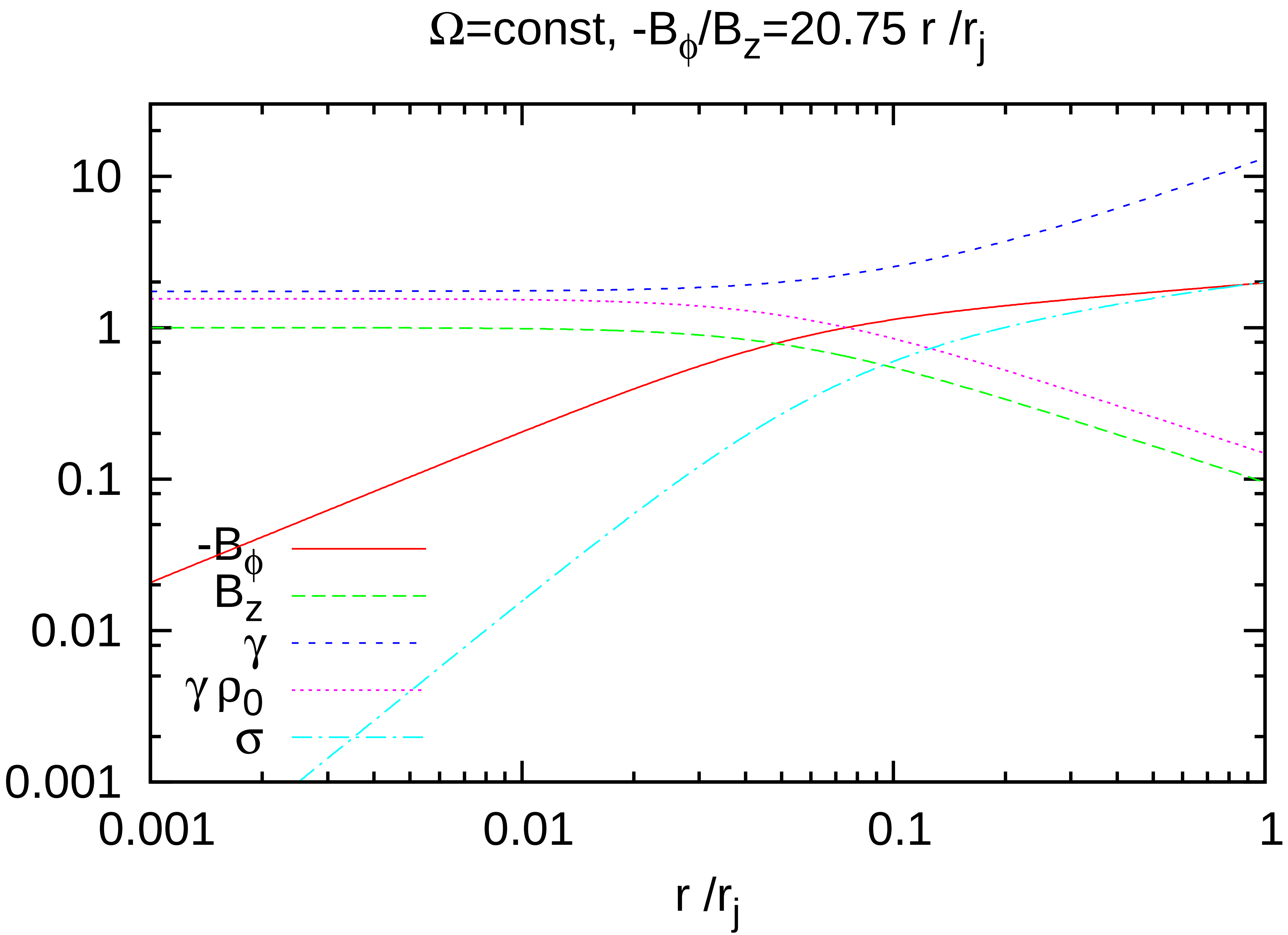

Ω=const, -B$_\phi$/B$_z$=20.75 r /r$_j$
10
1
0.1
0.01
0.001
0.001
0.01
0.1
1
r /r$_j$
-B$_\phi$
B$_z$
γ
γ ρ$_0$
σ

m=1, Ω=const

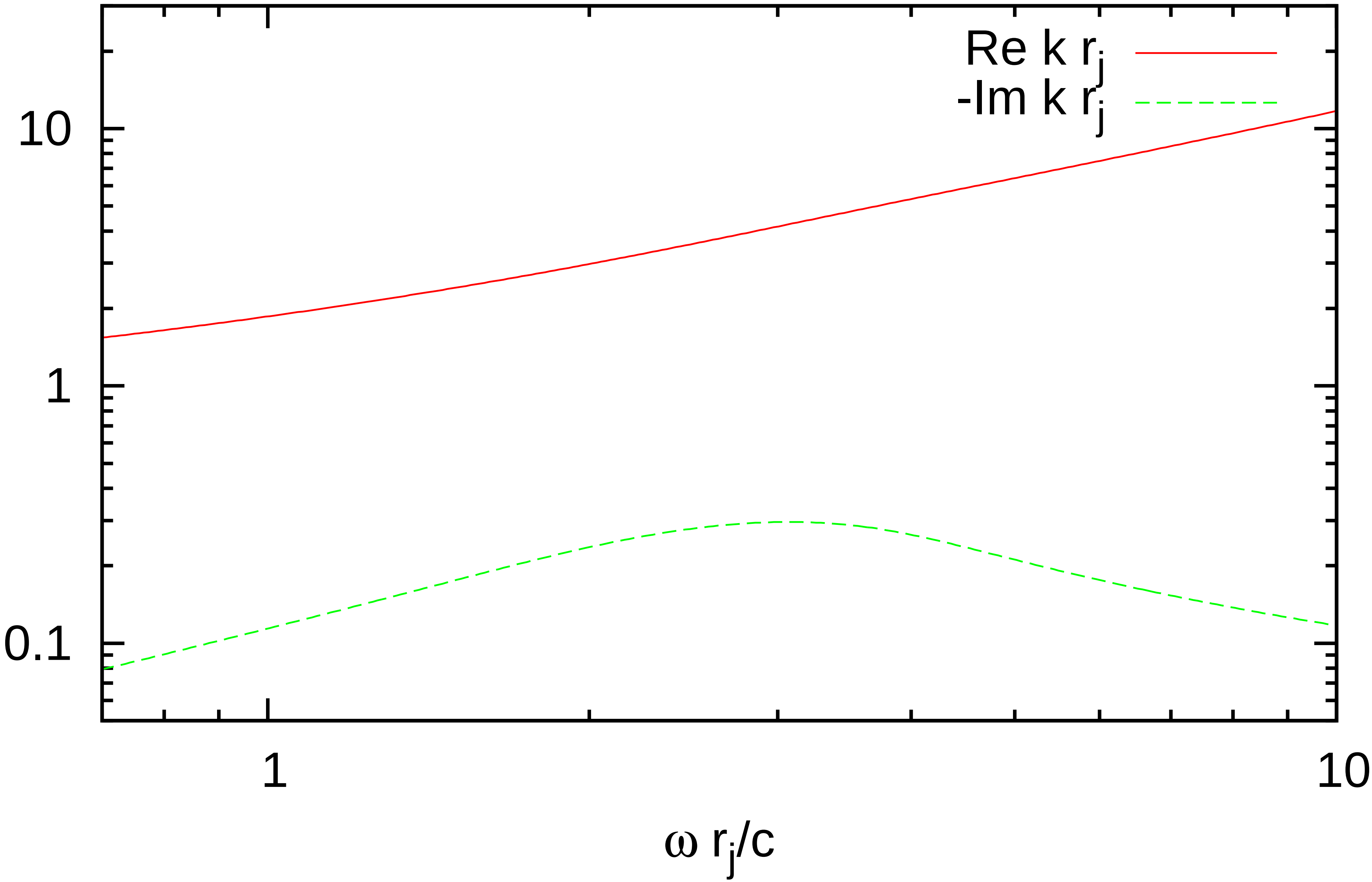

variable Ω

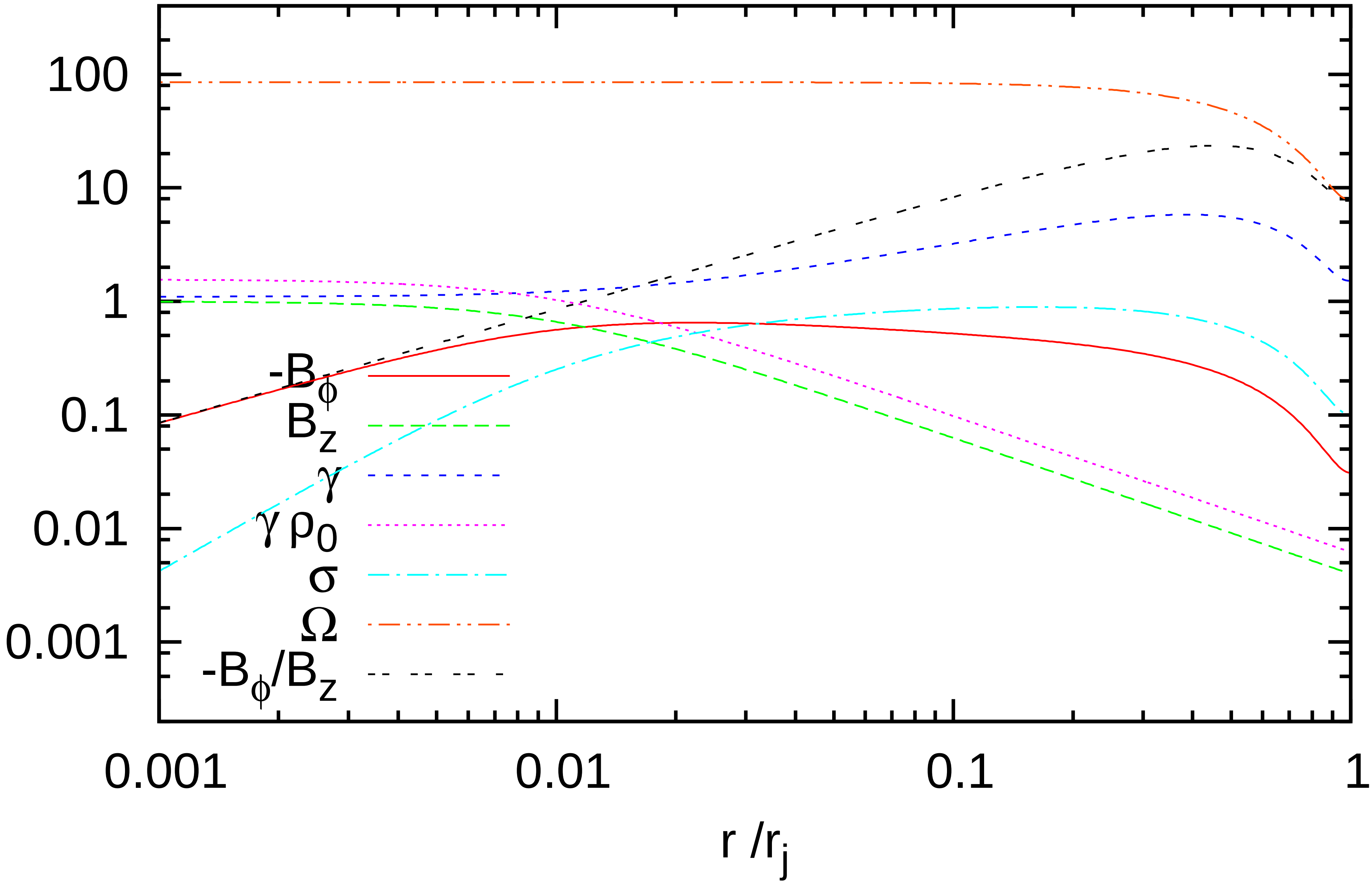

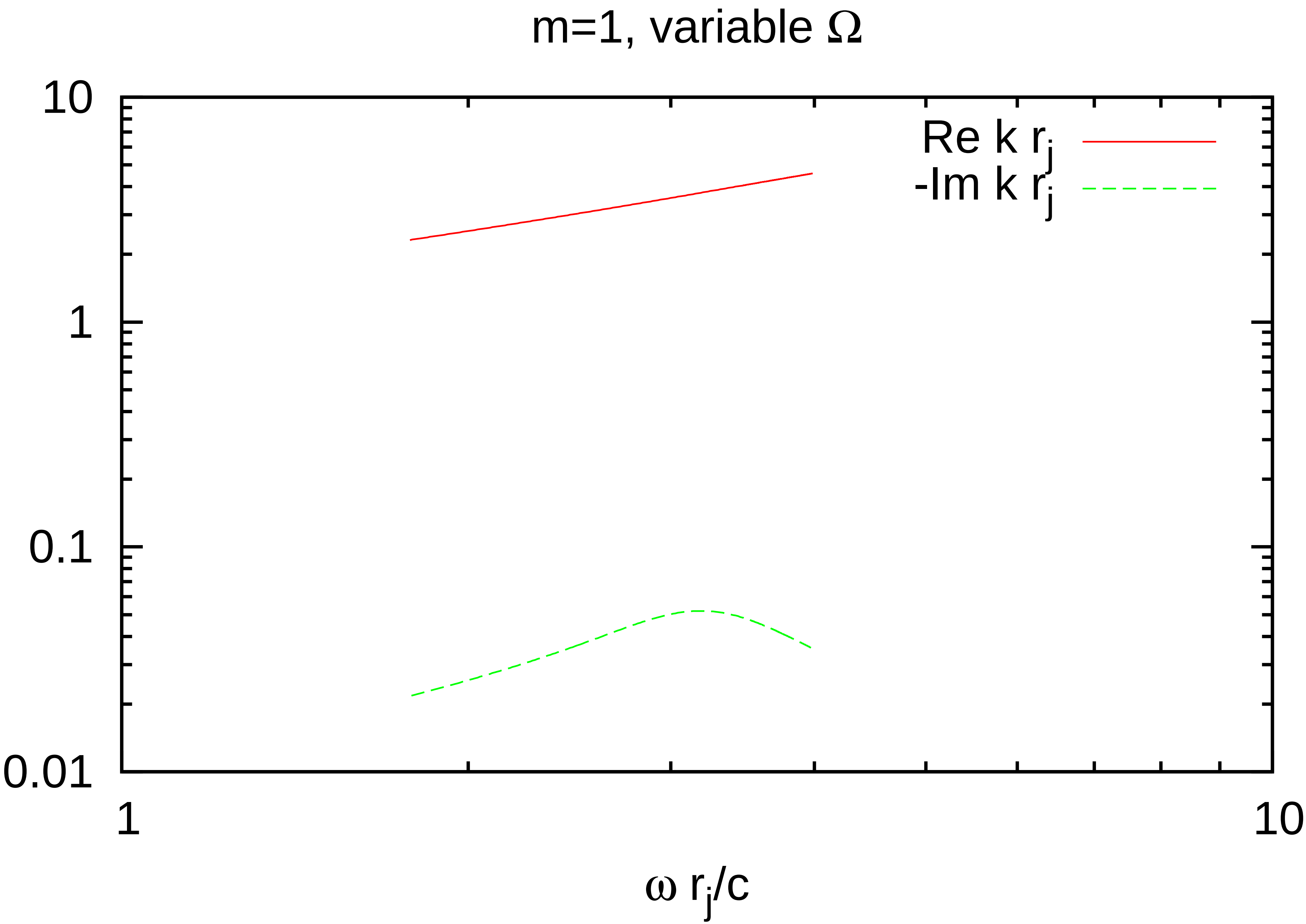
m=1, variable Ω
10
1
0.1
0.01
1
10
Re k r$_j$
-Im k r$_j$
ω r$_j$/c

Summary – Next steps

⋆ Kink instability in principle is in action.

⋆ Low $|B_\phi|/B_z$ and low σ (high γ) stabilize.

⋆ During the acceleration, growth time vs dynamical timescale?

⋆ Jets from accretion disks more stable?

- Explore the parameter space for kink and other modes
- colder/moving environment? other jet equilibrium models?
- comparison with numerical studies.

Rarefaction acceleration

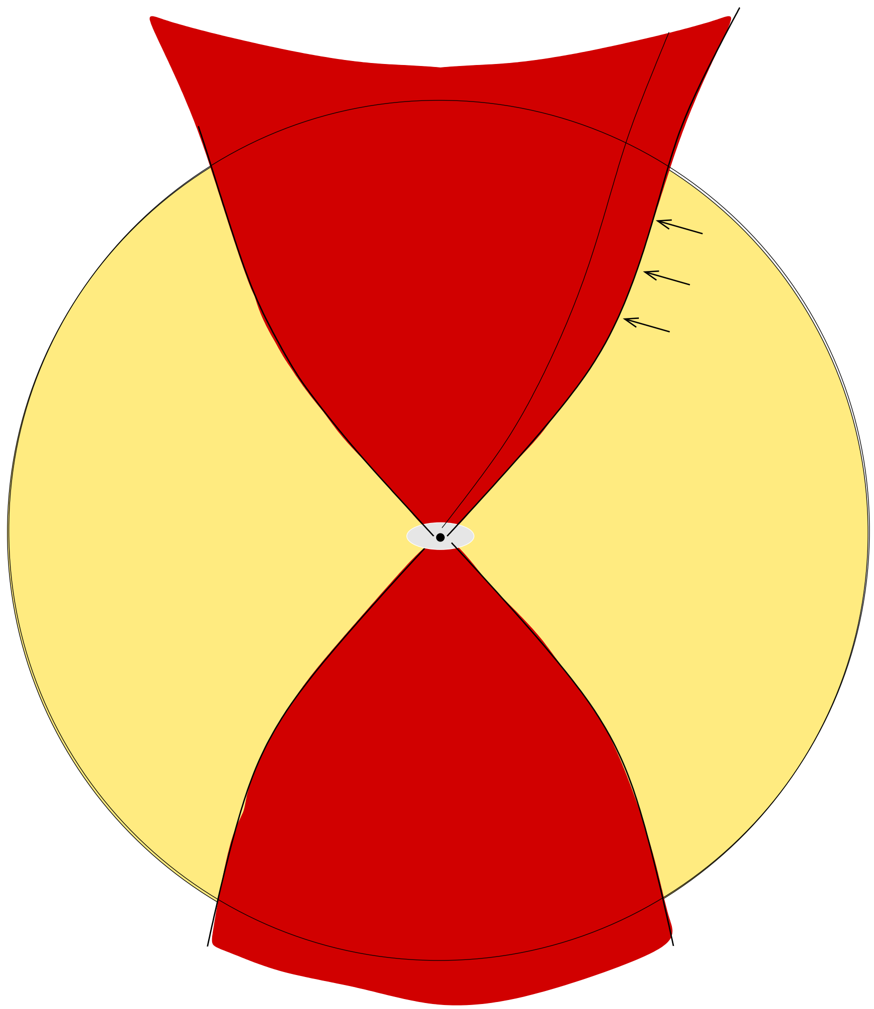

Rarefaction acceleration

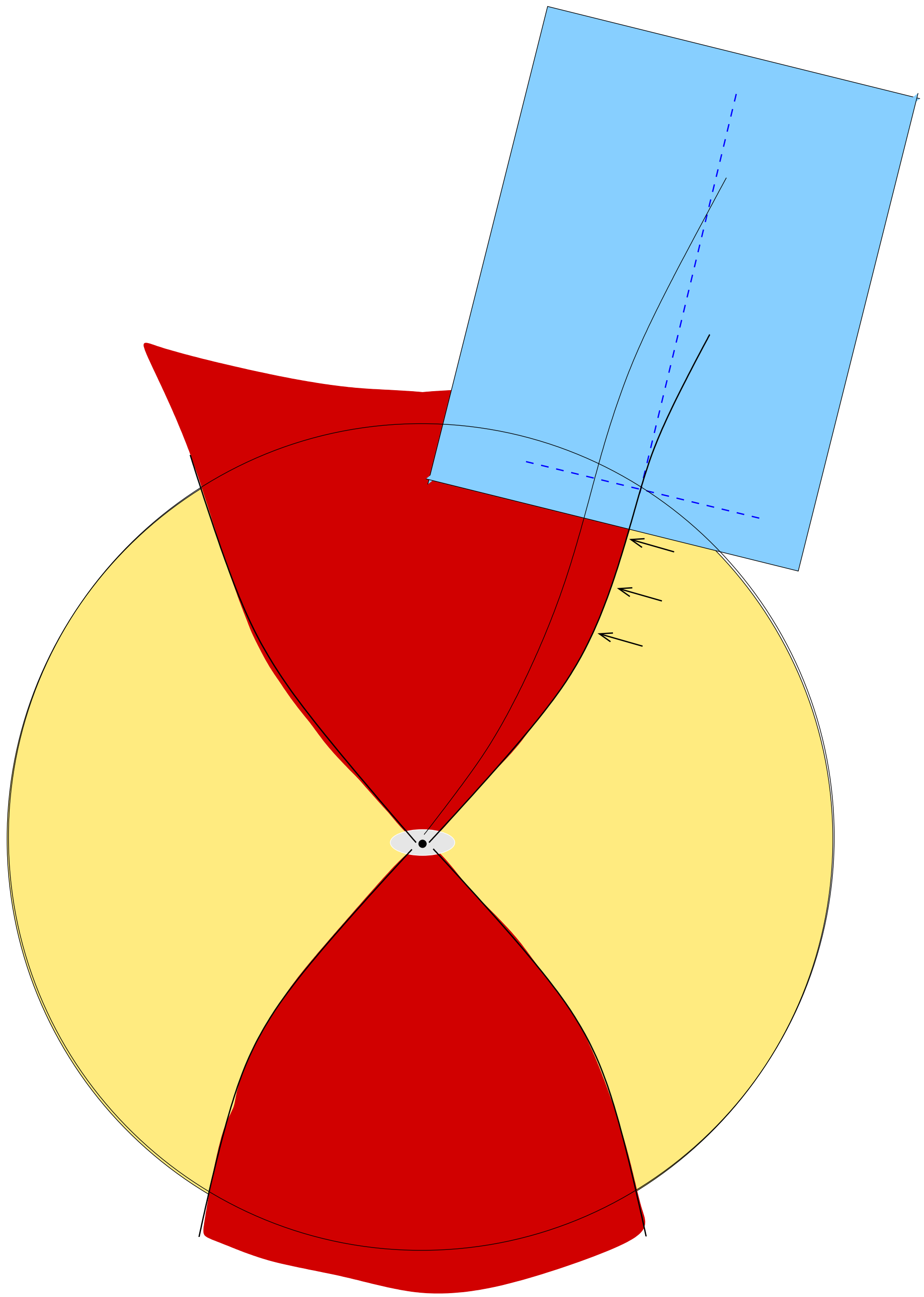

Rarefaction simple waves

At $t = 0$ two uniform states are in contact:

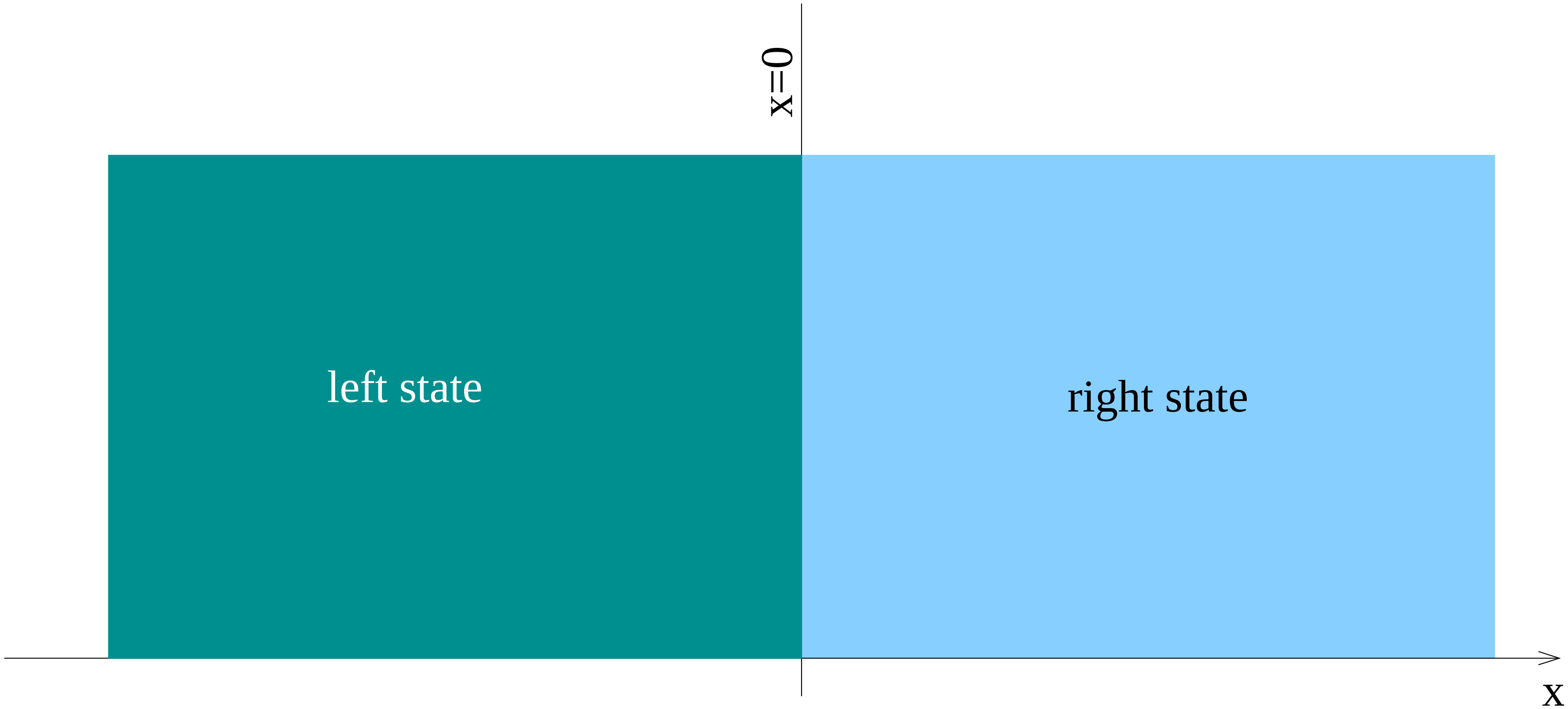

This Riemann problem allows self-similar solutions that depend only on $\xi = x/t$.

- when right=vacuum, simple rarefaction wave

At $t > 0$:

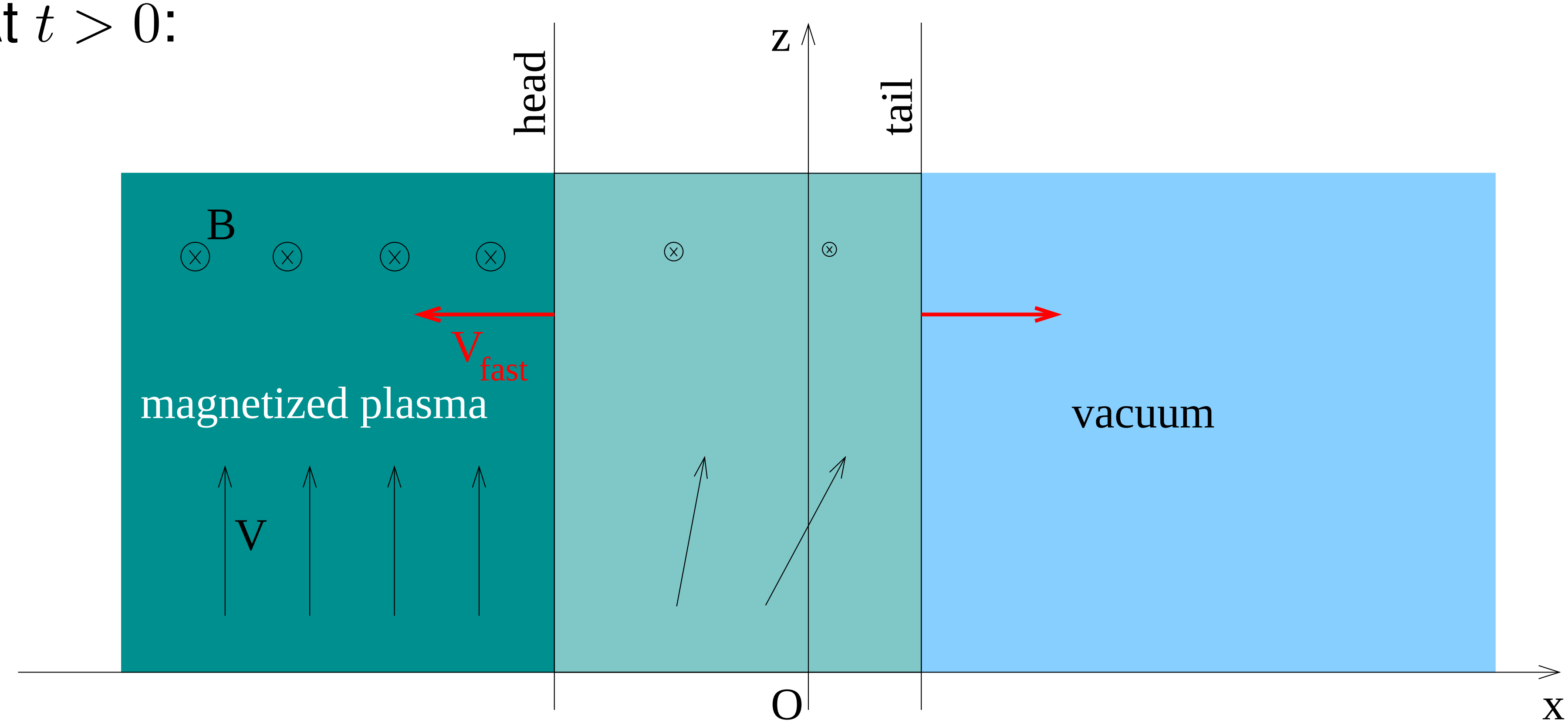

for the cold case the Riemann invariants imply

$$v_x = \frac{1}{\gamma_j}\frac{2\sigma_j^{1/2}}{1+\sigma_j}\left[1-\left(\frac{\rho}{\rho_j}\right)^{1/2}\right],\ \gamma = \frac{\gamma_j\,(1+\sigma_j)}{1+\sigma_j\rho/\rho_j},\ \rho = \frac{4\rho_j}{\sigma_j}\sinh^2\left[\frac{1}{3}\text{arcsinh}\left(\sigma_j^{1/2} - \frac{\mu_j}{2}\frac{x}{t}\right)\right]$$

$$V_{head} = -\frac{\sigma_j^{1/2}}{\gamma_j}, \qquad V_{tail} = \frac{1}{\gamma_j}\frac{2\sigma_j^{1/2}}{1+\sigma_j}, \qquad \Delta\vartheta = V_{tail} < 1/\gamma_i$$

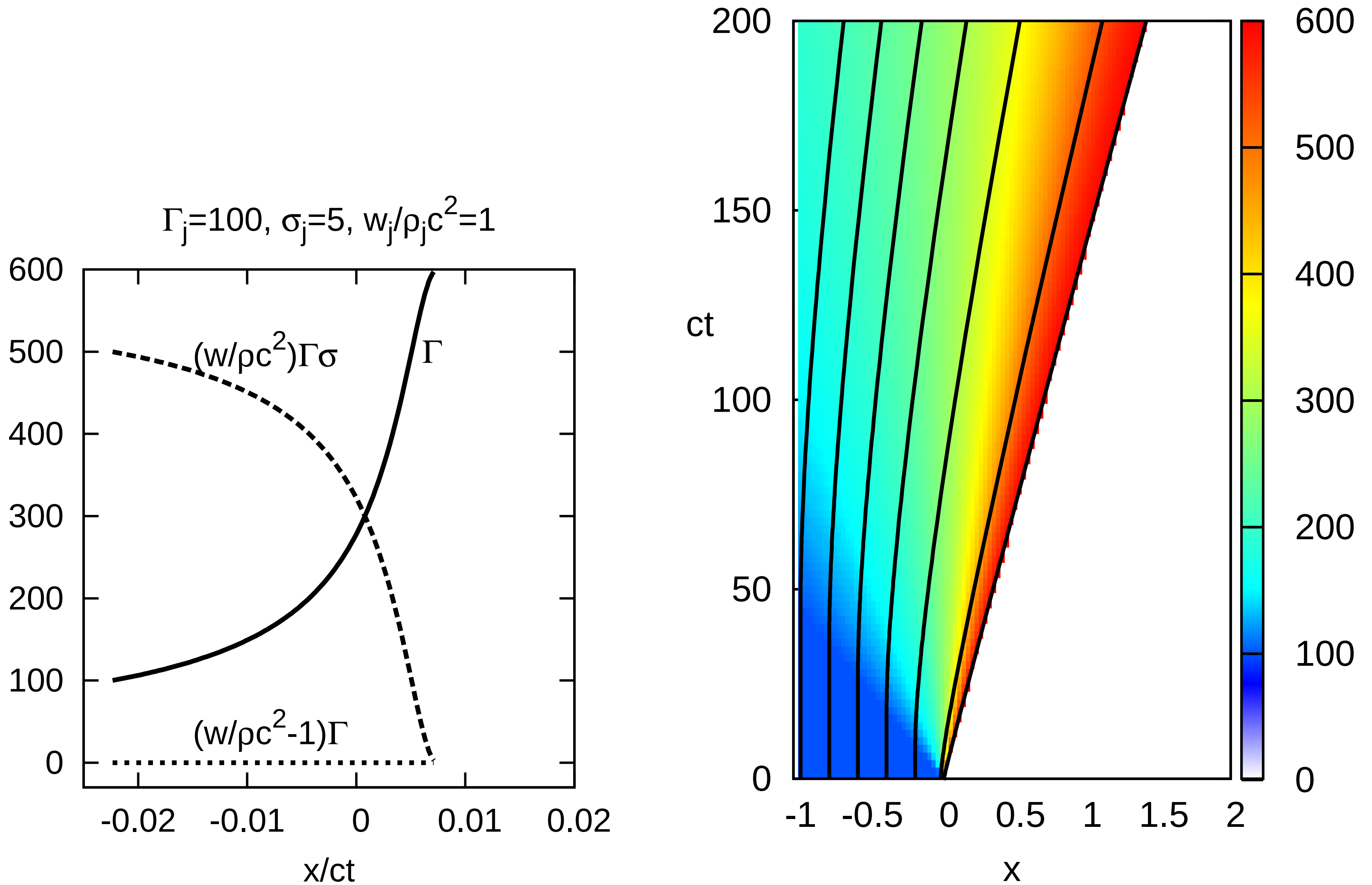

The colour image in the Minkowski diagrams represents the distribution of the Lorentz factor and the contours show the worldlines of fluid parcels initially located at $x_i = -1, -0.8, -0.6, -0.4, -0.2, -0.02, 0$.

Steady-state rarefaction wave

Sapountzis & Vlahakis (to be submitted)

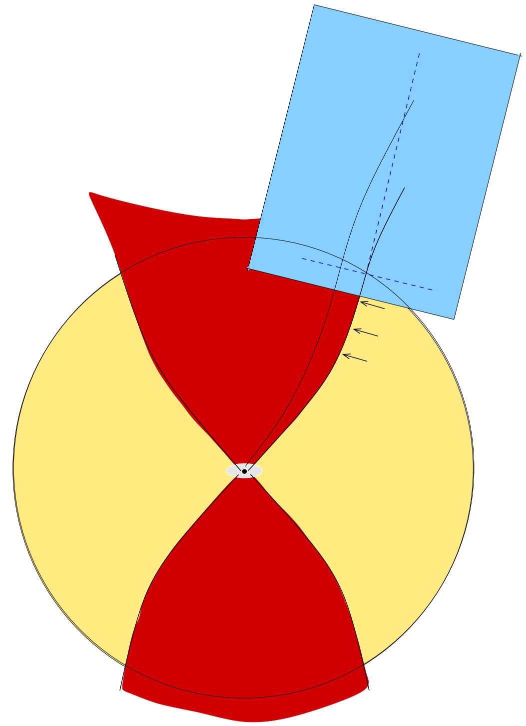

- "flow around a corner"
- planar geometry
- ignoring B_p (nonzero B_y)
- similarity variable x/z (angle θ)
- generalization of the nonrelativistic, hydrodynamic rarefaction (e.g. Landau & Lifshitz)
- in addition, allow for inhomogeneity in the "left" state

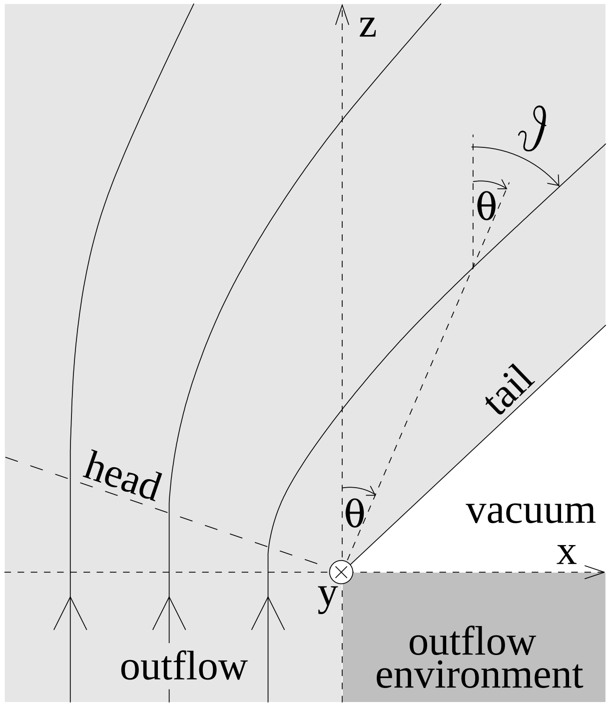

$$\gamma = \gamma_j \, \frac{1+\sigma_j}{1+\sigma_j(1-\vartheta/\theta_{\rm tail})^2}$$

$$\theta_{\rm head} = -\frac{\sigma_j^{1/2}}{\gamma_j}$$

$$\theta_{\rm tail} = \frac{2\sigma_j^{1/2}}{\gamma_j(1+\sigma_j)}$$

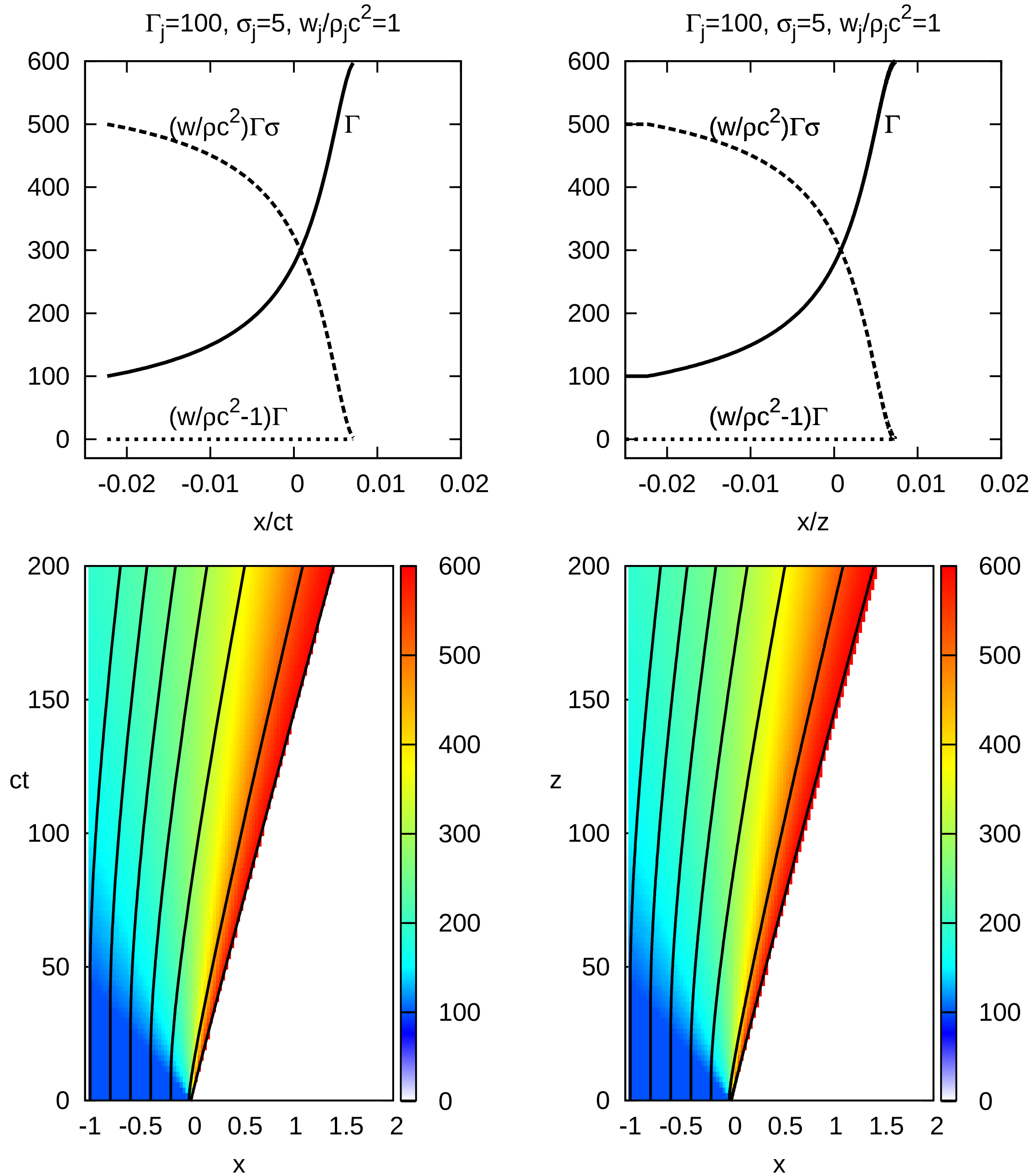

time-dependent (left) and steady-state (right) rarefaction (similar; $ct \rightarrow z$)

Axisymmetric model

Solve steady-state axisymmetric MHD eqs using the method of characteristics (Sapountzis & Vlahakis in preparation)

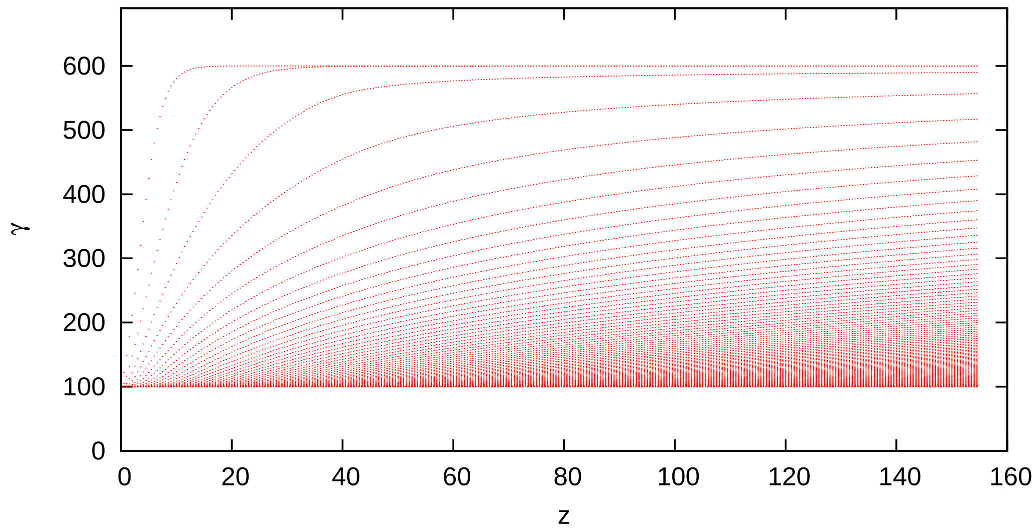

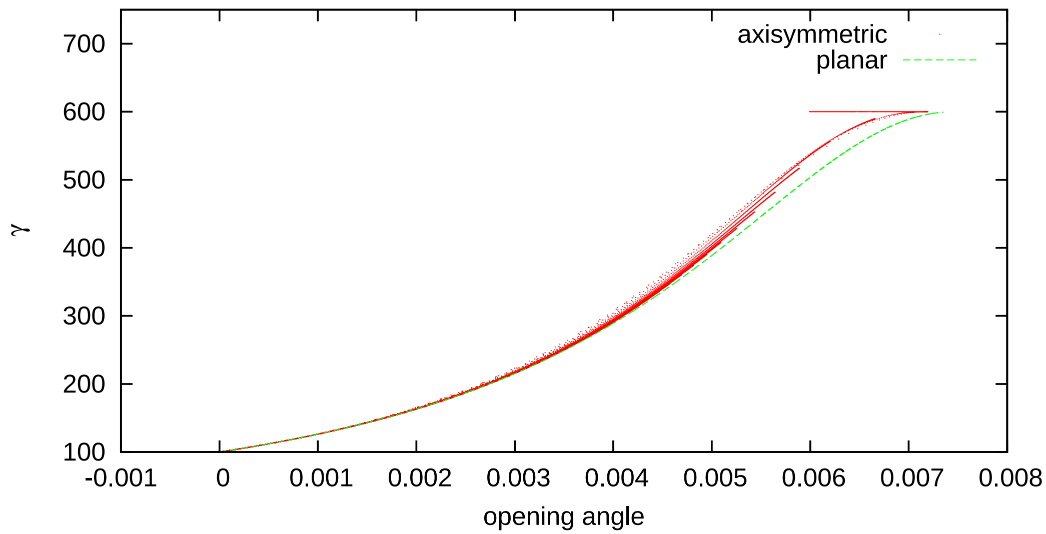

Summary – Next steps

⋆ The collimation-acceleration paradigm provides a viable explanation of the dynamics of relativistic jets
(similarly to non-relativistic ones)
(bulk acceleration up to Lorentz factors $\gamma_\infty \gtrsim 0.5 \frac{\mathcal{E}}{Mc^2}$)
BUT makes narrow jets with $\vartheta \sim 1/\gamma$ for high γ

⋆ Rarefaction acceleration

- further increases γ
- makes GRB jets with $\gamma\vartheta \gg 1$

⋆ Future work

- clarify the differences between 2D and 3D rarefaction cases
- apply other stratified jet models
- use realistic pressure distributions from stellar-evolution models

Acknowledgments

This research was partially funded by the University of Athens Special Account of Research Grants no 10812, and by the European Union (European Social Fund – ESF) and Greek national funds through the Operational Program “Education and Lifelong Learning” of the National Strategic Reference Framework (NSRF) - Research Funding Program: Heracleitus II. Investing in knowledge society through the European Social Fund.